Effect of the Preparation of Pt-Modified Zeolite Beta-Bentonite Extrudates on Their Catalytic Behavior in *n*-Hexane Hydroisomerization

Zuzana Vajglová,[†] Narendra Kumar,[†] Markus Peurla,[‡] Leena Hupa,[†] Kirill Semikin,[§] Dmitry A. Sladkovskiy,[§] and Dmitry Yu. Murzin*,[†][iD]

[†]Johan Gadolin Process Chemistry Centre, Åbo Akademi University, Biskopsgatan 8, Turku/Åbo 20500, Finland
[‡]University of Turku, Turku 20500, Finland
[§]St. Petersburg State Institute of Technology, St. Petersburg 190013, Russia

S Supporting Information

ABSTRACT: Four different types of shaped catalysts with controlled deposition of platinum and the same composition were prepared by extrusion of beta zeolite agglomerated with bentonite as an aluminosilicate clay binder. The catalysts were characterized using mechanical strength tests; scanning electron microscopy for morphology; transmission electron microscopy for porosity and periodicity; nitrogen physisorption for surface area, pore volume, and pore size distribution; and Fourier transform infrared spectroscopy using pyridine as a probe molecule to elucidate the presence, strength, and amount of Brønsted and Lewis acid sites. Elemental analysis was carried out using energy-dispersive X-ray microanalysis. Activity and selectivity of catalysts

in the isomerization of *n*-hexane were evaluated using a fixed bed reactor at 200−350 °C. At low temperature, the performance of metal/acid bifunctional shaped catalysis was strongly affected by the metal-to-acid site ratio. This ratio and the total acidity were strongly influenced by the preparation method of the shaped catalysts, while the textural properties were comparable. The highest conversion of *n*-hexane and selectivity to C$_6$ isomers (comprising all branched isomers, such as methyl pentane and dimethylbutane) was obtained with extrudates prepared via in situ synthesis with platinum located on the zeolite. The extrudates prepared in this way have the highest metal-to-acid site ratio and their closest proximity, albeit the lowest mechanical strength.
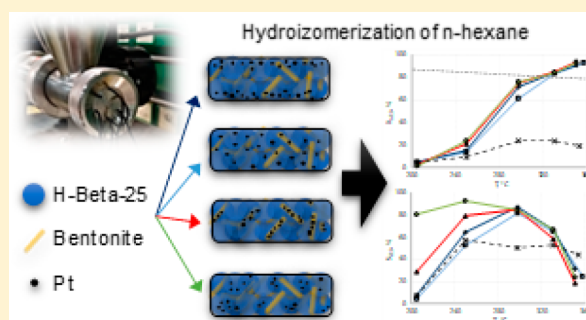
1. INTRODUCTION

Bifunctional catalysts typically contain both hydro/dehydrogenation and acid functions. In most catalytic processes, where such catalysts are involved, a noble metal (Pt, Pd) or a combination of non-noble metal sulfides from group VIA (Mo, W) and at least one from group VIIIA (Co, Ni) are chosen for hydro/dehydrogenation. As an acidic component, amorphous oxides such as silica−alumina, zeolites, or mesoporous aluminosilicates can be used. The metal can be either located within the pores of the acidic component and/or on the outer surface of the crystals, or supported on an inorganic binder in composite materials.[1−3] Bifunctional catalysts are used in many industrial processes of refining and petrochemical industries: reforming, hydrocracking of heavy oil cuts (e.g., vacuum gas oil) to produce diesel, dewaxing, hydroisomerization of C$_5$−C$_6$ *n*-paraffins to produce high-octane gasoline, C$_2$−C$_4$ aromatization, hydro-dealkylation or -isomerization of C$_8$ aromatic cuts, etc.[1−7]

Hydroisomerization of straight chain paraffinic hydrocarbons C$_5$−C$_6$ is one of the cheapest ways to increase the production of high-octane gasoline components with improved environmental characteristics while controlling formation of olefins or aromatics.[8−11] Linear alkanes such as *n*-hexane and *n*-heptane are characterized by low octane numbers, whereas (hydro)isomerization increases the octane numbers substantially if multibranched/dibranched isomers are obtained.[9]

Isomerization of *n*-alkanes over bifunctional metal/acid catalysts involves dehydrogenation of alkanes, skeletal isomerization of olefins and hydrogenation of the latter. Hydrogenation and dehydrogenation happen on the metallic sites, whereas isomerization or cracking require acid sites, thus diffusion of the olefinic intermediates from the metallic sites to acidic ones and back is important.[3,7,9,11−13] From this description of bifunctional catalytic transformations, it seems obvious that the catalyst properties, i.e., activity, stability, and selectivity, should depend on two main parameters: characteristics of the metal and acid sites and diffusional properties of
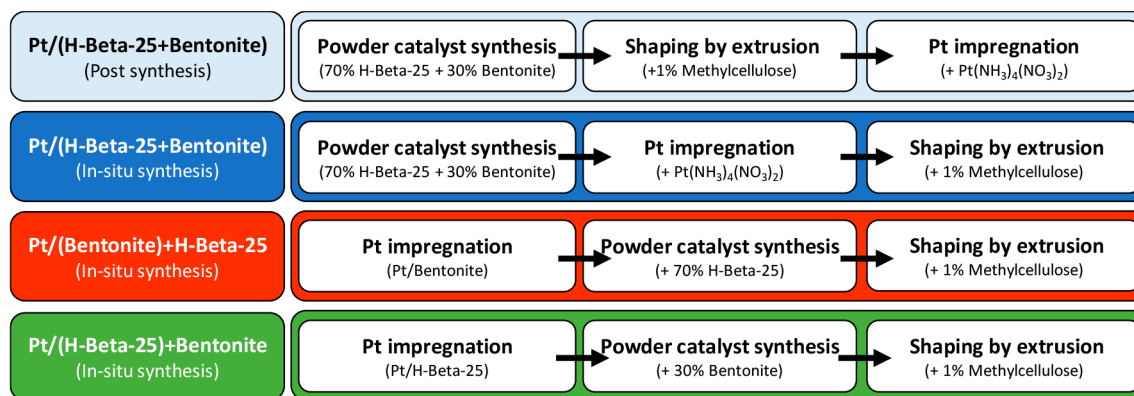
Figure 1. Procedures for synthesis of four different Pt extrudates.

the intermediates, influenced by the micropores of the acidic component.[3,6,7,9,12]

A proper choice of the hydro/dehydrogenation and the acidic component is dictated by the application. Acid sites and also micro- and mesoporosity of the catalyst play an important role in the catalyst selection. The most studied and industrially used zeolites are Y and ZSM-5 zeolites containing medium pores. Promising results were obtained for beta zeolites containing large pores. Studies focusing of hydroisomerization catalysts are often performed over bifunctional catalysts in the powder form because catalyst design is very complex and requires careful optimization, especially if a catalyst is to be used at an industrial level.[1,2,14−21]

For the latter purpose, catalysts are scaled-up, which necessitates application of binders (15−30 wt %) to make shaped bodies. Shaped catalysts in the form of granules, spheres or extrudates, being larger in size than powdered counterparts and mechanically stable, are needed to avoid extremely high pressure drops in fixed-bed reactors. For use as binders, commercially available natural clays, such as bentonite, attapulgite, and kaolin, are suitable. The overall aim of catalyst shaping is to achieve high catalytic activity and selectivity compared to the pristine zeolite, maintain chemical stability for prolonged use and achieve the required mechanical strength to resist attrition losses in industrial use.[1,17−20,22,23]

Catalyst shaping is thus a key step in catalyst preparation for large scale applications. The most commonly used techniques for shaping are tableting, spray-drying, granulation and extrusion.[24,25] Extrusion is probably the most widely applied unit operation among the ones mentioned above having an advantage of yielding high grain porosity and easy implementation. Shaping is not only crucial for the mechanical properties of catalysts but also for their catalytic performance.[25]

Unfortunately, detailed studies focusing on the shaped bifunctional catalysts are still lacking in the open literature.[1] Crushed shaped Pt catalysts (0.1−0.8 mm), where Pt was deposited on a zeolite[1,16,26] or a shaped support,[1,27,28] were applied in *n*-alkanes hydroisomerization (C$_7$−C$_{16}$). Lucas et al.[16] studied *n*-octane hydroisomerization over grinded shaped 1 wt % Pt catalyst comprising USY, mordenite, or beta zeolites and a bentonite binder and found a strong effect of the binder on catalytic performance. This influence was explained by alteration of the zeolite hydrogen transfer activity, metal/acid site balance, acid site density, and diffusional limitations after agglomeration. Mendes et al.[1] studied n-hexadecane hydro-

isomerization over grinded shaped Pt catalyst comprising USY zeolite and boehmite as a binder and on the contrary reported that the catalyst behaves rather as a mechanical mixture. According to Ramos et al.[28] the crushed shaped 1 wt % Pt catalyst, based on beta zeolite with bentonite as a binder, was the most selective for hydroisomerization, giving a higher iso-paraffins amount compared to other two zeolite-based catalysts (ZSM-5 and mordenite).

This work is aimed at shedding light on the parameters to be controlled during the scale-up of bifunctional catalysts from powder to shaped bodies. The focus is on both the impact of shaping on beta zeolite properties and on the method of preparation with controlled deposition of platinum. Bentonite often reported in the literature as a clay binder was applied because of its physical and chemical properties as well as a competitive price. Understanding of correlations between the physicochemical (surface, structural, textural, and morphological) properties and catalytic characteristics of noncrushed shaped Pt catalysts, could significantly contribute to the design of "ideal" (active, stable, and selective) bifunctional shaped catalysts indispensable to develop cleaner processes. As a model reaction isomerization of *n*-hexane was chosen.

2. EXPERIMENTAL SECTION

2.1. Preparation of the Shaped Pt Catalysts. The commercial beta zeolite NH$_4$-Beta-25 (SiO$_2$/Al$_2$O$_3$ = 25, CP814E) was obtained from Zeolyst International. The ammonium form was transformed to the corresponding proton form in a muffle oven using a step calcination procedure: initial temperature 250 °C (held for 50 min), increased at 4 °C/min to 400 °C and held at the final temperature for 4 h. As a binder aluminosilicate clay bentonite from VWR International was selected. Materials were crushed and sieved into a fraction <63 μm in a vibratory micro mill (Fritsch). A Pt-modified catalyst was prepared by a conventional evaporation−impregnation method. Tetraammoniumplatinum(II) nitrate (Pt-(NH$_3$)$_4$(NO$_3$)$_2$, ≥ 50.0% Pt basis, Sigma-Aldrich) was used as a platinum precursor.

The procedure of shaped Pt catalyst preparation includes three steps, namely catalyst synthesis, Pt impregnation and catalyst shaping. Different variations of the synthesis steps were used to prepare four different types (Figure 1). All catalysts were prepared with 70:30 ratio of H-Beta-25:bentonite and with a Pt nominal loading of 2 wt % in the final extrudates.

2.1.1. Powder Catalyst Synthesis. Catalyst synthesis included dry mixing, wet mixing, evaporation, drying, and

calcination. In the step of dry mixing, the zeolite and the binder were ground and mixed in a ball mill (Fritsch) for 4 h. The amount of the bentonite binder was 70% of H-Beta-25 and 30% bentonite. In the step of wet mixing, the aqueous solution was stirred with 50 rpm at ambient temperature for 24 h. In the subsequent steps, water was evaporated at 40 °C under vacuum and drying was carried out at 100 °C for 7 h. The calcination procedure was carried out at 500 °C for 4 h for catalysts without Pt and at 400 °C for 3 h for Pt- containing catalysts. Details of the synthesis of catalyst in the powder form are described in our previous publication.[22]

2.1.2. Pt Impregnation. Impregnation was carried out in a stirred bath containing 168 mL of 0.005 M aqueous solution of the metal precursor and 8 g of the catalyst support. The solution was rotated for 24 h at 60 °C, and subsequently water was evaporated at 40 °C under vacuum. The platinum catalyst was dried in an oven at 100 °C for 24 h, calcined at 400 °C for 3 h in a muffle oven, and reduced at 350 °C for 2 h by 40 mL/min H_2.

2.1.3. Catalyst Shaping. The slurry for the extrusion device applied in catalyst shaping (TBL-2, Tianjin Tianda Beiyang Chemical Co. Ltd., China) was prepared in the weight ratio 44.5/54.5/1.0 for the catalyst powder/distilled water/methyl-cellulose. Methylcellulose as an organic binder (viscosity: 4,000 cP, Sigma-Aldrich) was added into the mixture for better rheological properties of the final slurry. The extrudates (Figure 2) were formed into the cylindrical shape with a
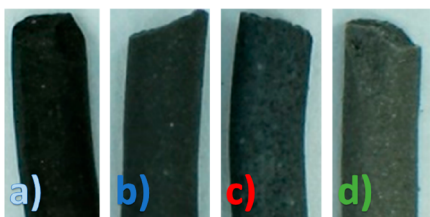

Figure 2. Pt extrudates of beta zeolite agglomerated with bentonite as a clay binder. The extrudates differ in the way Pt was introduced: (a) after extrusion or prior to extrusion on (b) zeolite and binder, (c) binder, (d) zeolite.

diameter of 1.4 mm at a continuous velocity of 1400 rpm (Figure 3). The extrudates were dried, calcined, and reduced at the conditions described above. Before reduction, the extrudates were cut to the length of ca. 1 cm.

Figure 3. Photos of the extruder: (a) screw; (b) shaping of Pt ncatalyst.

2.2. Characterization of Shaped Pt Catalysts.
2.2.1. Rheology and Calculations of Extruder Properties. The shear rate describing the velocity gradient between two surfaces moving at different speeds (e.g., screw and barrel wall), is a function of the screw outside diameter, screw speed, and gap. It was calculated to be 327 s^{-1} according to the following equation:[29]

$$\text{shear rate}(\text{s}^{-1})$$
$$= \frac{[\pi \cdot \text{screw diameter (mm)} \cdot \text{screw speed (rpm)}]}{[\text{gap (mm)} \cdot 60 \text{ (s/min)}]} \quad (1)$$

where the gap is defined as the distance between the moving surfaces (e.g., the mechanical clearance between the screw and barrel). The linear catalyst formulation rate was ca. 12 cm/min, giving extrudates of 1.4 mm in diameter after passing through holes of 1.5 mm.

2.2.2. Scanning Electron Microscopy (SEM) and Energy-Dispersive X-ray Microanalysis (EDX). Morphological studies were performed by scanning electron microscopy. A scanning electron microscope (Zeiss Leo Gemini 1530) was used for determination of the crystal morphology. Elemental analysis of microporous materials was done by energy-dispersive X-ray microanalysis using the same instrument.

2.2.3. Transmission Electron Microscopy (TEM). Particle size and porosity of the materials were characterized by transmission electron microscopy (JEOL JEM-1400Plus) using imaging and electron diffraction functions. The samples were prepared by blowing a powder on the TEM grid with a pipet. Determination of Pt particle size and the intercluster distances was done from the TEM images using the ImageJ program.[30] For each sample, the median from 100 and more measurements was calculated.

2.2.4. Nitrogen Physisorption. Nitrogen-physisorption using Sorptometer 1900 (Carlo Erba Instruments) was performed to determine the textural properties of microporous materials. The samples were outgassed at 150 °C for 3 h before each measurement. The Dubinin equation and the Horvath–Kawazoe method[31] were used for calculation of the specific surface area and the pore volume, respectively.

2.2.5. Fourier Transform Infrared Spectroscopy (FTIR). The amount of Brønsted and Lewis acid sites was quantified by Fourier transform infrared spectroscopy using pyridine (≥99.5%) as the probe molecule (with ATI Mattson FTIR Infinity Series spectrometer). The samples were pressed into thin pellets (10−20 mg) and placed in the measurement cell. Prior to pyridine adsorption, the samples were outgassed under vacuum (0.08 mbar) at 450 °C for 2 h and the background spectra were recorded at 100 °C. Pyridine was adsorbed at 100 °C for 30 min and the spectra were recorded at 100 °C after heating the sample to 250, 350, and 450 °C, respectively. The Lewis acidity was determined from the adsorption band at 1450 cm^{-1} and the Brønsted acidity from the adsorption band at 1550 cm^{-1} using the molar extinction parameters previously reported by Emeis.[32]

2.2.6. Mechanical Strength Test. L&W crush tester with two parallel plates (SE 048, Lorentzen & Wettre, Sweden) was used to detect the force needed for an extrudate to collapse. Two plates were moved toward each other using a hydraulic device, recording the pressure at which the catalyst extrudates were broken. The moving speed of the plates was 1 mm/min. The mechanical strength of the extrudates (10 mm in length and 1.4 mm in width) was determined in the vertical and horizontal positions (Figure S1). For every sample, an average of ten crush tests in each position were calculated.

2.3. Catalytic Tests. Isomerization of *n*-hexane (Figure 4) was used as a model reaction to characterize activity and selectivity of shaped Pt catalysts. The reactant contained a small amount (1%) of benzene to elucidate also ability of the catalysts in hydrogenation of the aromatic ring, subsequent
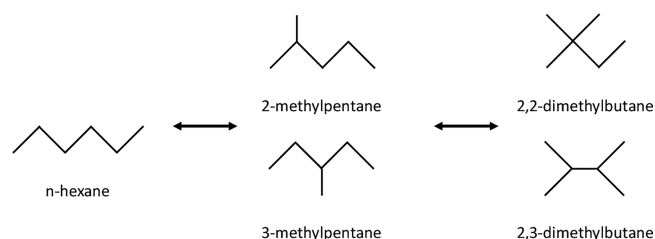
Figure 4. Isomerization of *n*-hexane.

ring contraction and ring opening (Figure 5). The reaction was carried out in a fixed bed reactor (12 mm in diameter, catalyst zone of 70 mm, thermocouple pocket of 3 mm, reactants flow top to bottom, a turbulizer upstream catalyst). The reaction conditions were: pressure 17 barg, reaction temperature 205–358 °C; hydrogen flow rate 180 mL/min and feedstock flow rate 0.24 mL/min. The catalysts in the amounts of 3 g (7.3 cm^3) were activated in situ at 350 °C in the nitrogen flow rate of 122 mL/min under 10 bar during 1 h. Reduction of the catalysts was carried out in the hydrogen flow rate under the same conditions as the catalyst activation. The products were drained from the separator used to collect the sample, which required 30 min.

3. RESULTS AND DISCUSSION

3.1. Characterization Results of Shaped Pt Catalyst.

3.1.1. Elemental Analysis. Results from elemental analysis of the samples from each step of shaped Pt catalyst preparation are summarized in Table S1. In the case of extrudates, only the catalyst surface was analyzed. In the pristine methylcellulose, Na and Cl were observed in amounts of 0.28 and 0.21 wt %, respectively. The purpose of using organic binder methylcellulose is to influence the viscosity and rheological properties of the H-Beta-25+Bentonite mixture for extrusion. No methylcellulose was found in the final extrudates, which confirms that after extrudate synthesis, the organic binder methylcellulose was removed from the matrix during calcination at the elevated temperature (500 °C).[33]

Changes of the mixture composition in H-Beta-25 with 30% of bentonite as well as the Pt concentration in the catalysts before and after extrusion can be related to inhomogeneous mixing of the beta zeolites and the bentonite binder. This, in combination with a lower accuracy of the utilized EDX method, related to a small area used for detection and a low concentration of impurities originating from bentonite (MgO, K$_2$O, and Fe$_2$O$_3$), can give different results.

A high Pt content of 8.33 wt % observed on the surface of Pt/(H-Beta-25+Bentonite) extrudate (prepared via the post synthesis with a Pt nominal loading of 2 wt %) indicates that it is of the egg shell type with the active metal located on the

outmost layer of the catalyst. On the contrary, the Pt content of 2.31 wt % observed on the surface of Pt/(H-Beta-25+Bentonite) extrudate (prepared via in situ synthesis with a Pt nominal loading of 2 wt %) indicates that Pt is uniformly distributed across the extrudates.

To confirm this hypothesis about distribution of Pt in extrudates, X-ray mapping was done for the cross-section view of 2% Pt/(H-Beta-25+Bentonite) extrudates (Figure S2, top of the extrudate after the metal introduction). The samples were mounted in resin and dry grinded. It was observed that Pt distribution is somewhat different in both extrudates. A denser distribution of Pt on the outer layer of an extrudate (cross-section view) was observed in the Pt catalyst prepared via the post synthesis (Figure S2a). These results are consistent with the results of elemental analysis.

The images from optical microscopy (Figure S3) also confirmed the results of elemental analysis. In the longitudinal cross section view of the extrudate prepared via the post synthesis, a penetrated Pt layer with an average thickness of 60 µm was visible (Figure S3, bounded by dashed line). It is in line with the work of Delmon et al.,[34] who proposed that protons from the Pt precursor attack the surface upon penetration of the extrudates by the liquid. The sites created by this attack are situated in the outer layer of the extrudates and serve as strong adsorption sites for Pt. A homogeneous Pt distribution in the extrudates prepared via post synthesis method can be obtained when an additional acid is present in the impregnation liquid. This acid can create additional adsorption sites onto the extrudate both for Pt and the acid anions throughout the particle. Because of the adsorption competition between both anions, a homogeneous Pt distribution can be obtained. This phenomenon where Pt is mostly deposited on the edges of the extrudate instead of being uniformly distributed was also reported by de Mendes et al.,[1] but only for a much lower Pt content (0.07% Pt/HUSY +Al$_2$O$_3$).

The results of 2.3–3.4 wt % Pt in extrudates prepared via in situ synthesis are close to the nominal loading (2 wt % Pt), indicating that the impregnation method used for the metal introduction was successful. A slightly higher measured value can be related to the precision of analysis.

3.1.2. Morphology, Porosity, and Periodicity. The SEM images (Figure S4) show that the structure of H-Beta-25 zeolites and bentonite was not changed after Pt impregnation. Just like pristine materials,[22] Pt/H-Beta-25 contains mainly aggregates of spherical crystals, whereas the structure of Pt/bentonite mainly consists of fibers and platelets with sharp edges. The SEM images (Figure S4) also confirm interfacial interactions in the synthesized powder materials and in Pt extrudates where the morphological characteristics cannot be clearly attributed to either of the neat materials. SEM images
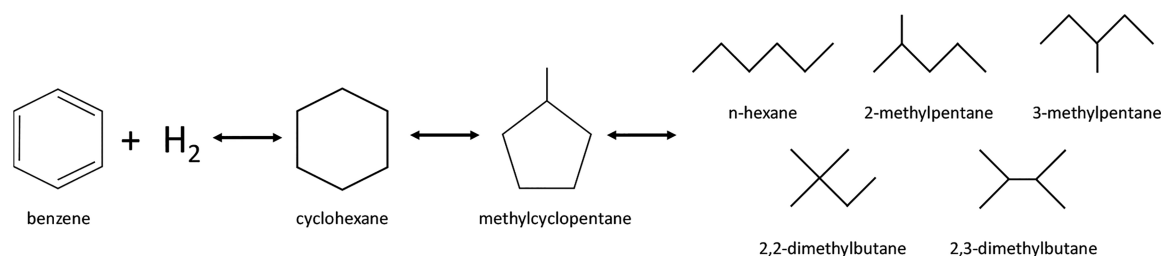

Figure 5. Hydrogenation of benzene with ring opening of cyclohexane.

clearly demonstrate morphological changes during each step of the shaped catalyst preparation.

In the case of extrudates prepared via post synthesis, a strong compact structure of the extrudates with significant smooth bentonite areas (black spots) is observed. For extrudates prepared via in situ synthesis, the beta zeolite was locally deposited on bentonite. The neat structures of beta zeolite and bentonite were also observed here, which were largely interconnected with a smooth bentonite bridge. In all cases, the structure was more compact and smoother because of extrusion. The average diameter of all extrudates determined by SEM was 1.38 ± 0.01 mm.

In line with the results of elemental analysis, the SEM results also confirm that methylcellulose was burned and removed from the extrudates during calcination. No morphology features of pristine methylcellulose (Figure S5) were observed in any of the final extrudates.

Pt dispersion (Figure S6) was 19, 33, 44, and 70% for Pt/(H-Beta-25+Bentonite, post), Pt/(H-Beta-25+Bentonite, in situ), Pt/(H-Beta-25)+Bentonite and Pt/(Bentonite)+H-Beta-25 extrudates, respectively. Pt dispersion was calculated on the basis of the average Pt particle size determined by TEM.[35] The samples were mainly monodisperse. Larger clusters were sporadically observed only for Pt/(Bentonite)+H-Beta-25. It was also confirmed that Pt is localized exclusively on bentonite for Pt/(Bentonite)+H-Beta-25, whereas in the case of Pt/(H-Beta-25)+Bentonite, location of Pt was on H-Beta-25. A decrease in Pt particle size after extrusion was observed in all types of extrudates. A plausible explanation for a decrease in the Pt particle size after extrusion could be variations in the location of Pt particles in beta zeolite and the bentonite binder. Furthermore, during calcination of extrudates and removal of the organic binder methylcellulose, the latter at elevated temperature can act as a reducing agent for Pt particles, enhancing dispersion of Pt and formation of small Pt particles. The smallest Pt particle sizes of 1.6 nm were measured for Pt/(Bentonite)+H-Beta-25 while the largest Pt particle sizes of 7.4 nm were observed for Pt/(H-Beta-25+Bentonite) prepared via post synthesis. Pt metal particles with a size of 2.5–3.5 nm were reported for the Pt powder catalyst containing Y zeolite and Al_2O_3 binder.[13]

The shortest average distance between two Pt sites of 4 nm was measured for Pt/(Bentonite)+H-Beta-25 extrudates. For other types of extrudates, the distance was comparable, i.e., 12, 14, and 16 nm for Pt/(H-Beta-25)+Bentonite, Pt/(H-Beta-25+Bentonite) prepared via post synthesis and in situ synthesis, respectively.

3.1.3. Textural Properties. A detailed analysis of the textural properties of the catalysts (Table S2) shows that the preparation method of the shaped catalysts had a negligible influence on the final specific surface area and extrudate porosity. For all shaped Pt catalysts, the specific surface area and the micropore volume are ca. 34% lower compared to the pristine H-Beta-25 zeolite and ca. 56% lower in terms of meso- and macropore volume.

3.1.4. Brønsted and Lewis Acid Sites. According to the previous studies,[22,36,37] the binder presence can decrease the acidic properties of a zeolite as a result of changes in the solid-state ion exchange between zeolite protons and clay sodium. Bentonite is a rich source of Na^+ cations, which are also weak acid sites.[22,38] Although a part of them is removed and substituted by H^+ during the reincorporation of the acid function, Na^+ cations remaining in the sample alter the acid

sites density because at least some of the weak sites can be attached to them.[16] When using bentonite as a binder, the technical catalyst showed a decreased bio-oil deoxygenation activity, which was assigned to the loss of most of ZSM-5 acidity by ion-exchange with Na^+ cations from the clay.[39] In bentonite besides Na, there are other cations such as Fe, Mg, K, and Ca, the presence of which can inhibit catalytic activity.

This is also confirmed by the results in Table S3, where the composite material (H-Beta-25 with 30% of bentonite without Pt) exhibited a lower total acidity compared to the theoretical value (values in brackets). The acidity was similar after extrusion and also after Pt impregnation being in line with the literature.[1] For in situ prepared Pt/(H-Beta-25+Bentonite) and Pt/(Bentonite)+H-Beta-25, there was an increase in weak and medium acidity accompanied by a decrease in strong acidity after extrusion. On the contrary, for Pt/(H-Beta-25)+Bentonite, the opposite trend was observed. The total acidity was increased after extrusion for Pt/(H-Beta-25+Bentonite) prepared via in situ synthesis, whereas for Pt/(Bentonite)+H-Beta-25 and Pt/(H-Beta-25)+Bentonite, the total acidity decreased after extrusion. It follows that the influence of extrusion on the total acidity requires further investigation to establish parameters, which determine the total as well as Brønsted and Lewis acidity (Table S3). At the same time, it can be unequivocally concluded that Pt deposition significantly affects acidity, which will be discussed in Section 3.2 considering the decreasing distance between Pt and zeolitic sites.

Kubicka et al.[40] stated that interactions between platinum and the support are mutual, i.e., that the support affects the properties of platinum and that, at the same time, the support properties are influenced by platinum. In line with the literature,[40] a lower acidity was observed for the Pt-modified zeolite as compared to the pure zeolite. In contrast, for the Pt-modified binder, acidity was higher than for neat bentonite.

It is worth noting there was a significantly lower measured value of the total acidity than the expected one for Pt/(Bentonite)+H-Beta-25, whereas for Pt/(H-Beta-25)+Bentonite, the experimental value matched the theoretical one. The theoretical values were calculated based on the contribution of nonagglomerated components. It follows that another decrease in total acidity was achieved because of Pt−acid site interactions during Pt/binder and H-Beta-25 mixing, whereas these interactions were insignificant during mixing Pt/H-Beta-25 and bentonite.

3.1.5. Crushing Strength. It was revealed that the mechanical strength of shaped 2% Pt catalysts could be correlated with the Pt loading (Figure S7), i.e. the strength of the extrudate increases with increasing Pt concentration. Interestingly that in comparison with the metal-free extrudates (full black line, Figure S7), the mechanical strength in a vertical position was higher for extrudates with a random deposition of Pt and lower when platinum was deposited exclusively on H-Beta-25 or on bentonite. In the case of the horizontal position, the mechanical strength of metal-free extrudates was always higher than for Pt extrudates. These results could be correlated to the total pore volume of extrudates, as the mechanical strength of the extrudates in the vertical position linearly decreases with increasing porosity (Figure S8a). For the mechanical strength of extrudates in the horizontal position, the effect of porosity is not that apparent (Figure S8b).

Compared to commercial Al_2O_3 extrudates (BDH Ltd., Poole), the extrudates prepared in the current work had ca. 4−
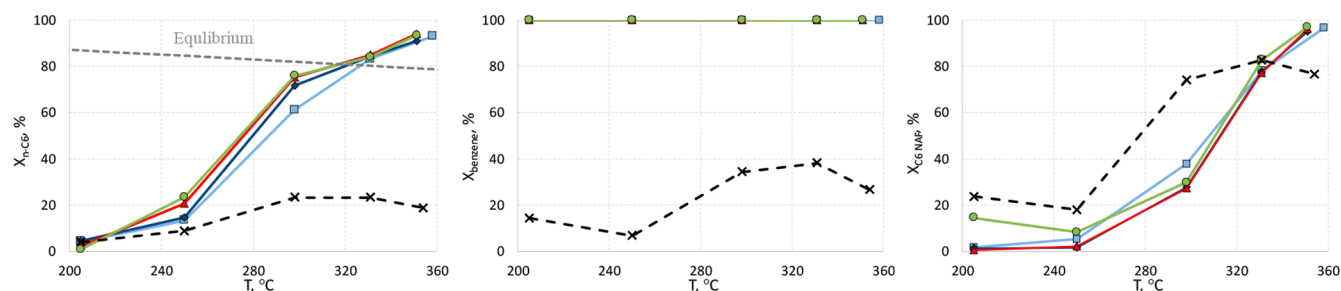
Figure 6. Conversion of (a) *n*-hexane and (b) benzene; (c) C_6 naphthene ring opening as a function of temperature. Symbols: 100% H-Beta-25 (CP814E, powder), black cross; Pt/(H-Beta-25+Bentonite), 2% Pt extrudate (post synthesis), blue square; Pt/(H-Beta-25+Bentonite), 2% Pt extrudate (in situ synthesis), blue diamond; Pt/(Bentonite)+H-Beta-25, 2% Pt extrudate (in situ synthesis), red triangle; Pt/(H-Beta-25)+Bentonite, 2% Pt extrudate (in situ synthesis),− green circle.

5 fold lower mechanical strength (Table S4). However, this strength is still sufficient for catalytic applications. All Pt catalysts tested in this work as extrudates kept their shape and length also after the reaction. Compared to the literature data,[21,41−44] it is noticeable that at least the metal-free extrudates prepared in the current work reached the same or higher values (Table S4). The data on the crushing strength of shaped bifunctional catalysts are rather scarce diminishing possibilities of comparison with the results of the current study. Sulfated Zr with 30% boehmite extrudates exhibited similar or much better mechanical strength (3.8−10.3 ± 0.3 MPa)[24] compared to shaped Pt catalysts prepared in this work.

Mechanical strength of the extrudates is influenced by the binder type used for their synthesis, ratio of the support and the binder used for preparation of extrudates, the particle size and calcination. Because several parameters are important for making mechanically strong extrudates, understanding stability and strength of extrudates requires separate research.

3.2. Activity and Selectivity of Shaped Pt Catalysts in Isomerization of *n*-Hexane. For a pristine commercial H-Beta-25 catalyst in the powder form and four different types of shaped catalysts with controlled deposition of platinum and the same composition, activity and selectivity were measured in isomerization of *n*-hexane (Figure 6a) containing 1% benzene, which underwent hydrogenation and ring opening (Figure 6b, c). Definitions of calculations are provided in the Supporting Information. The mass balance closure was ca. 99% with the errors of GC analysis being in the range of ca. 1%.

Significant differences in n-C_6 hydroisomerization and benzene hydrogenation with ring opening were observed below 330 °C (Figure 6). Conversion of benzene was 100% for all shaped Pt catalysts at the same being maximum 40% for pristine H-Beta-25 in the whole temperature range (Figure 6b). Deactivation was observed only for pristine H-Beta-25 catalyst in the powder form, which can be explained by coke accumulation and catalyst pores blocking.[7,9] All types of Pt extrudates were catalytically stable under all tested reaction conditions.

At 250 °C, the largest differences were observed in n-C_6 conversion and at the same time in selectivity (Table 1). The extent of isomerization reflects the fraction of high-octane number component-2,2-dimethylbutane (RON = 92) in the isomerizate and determines its octane characteristics. With increasing temperature, there was an increase in both conversion of *n*-hexane and selectivity to dimethylbutane. Upon further temperature elevation, however, cracking is enhanced, forming C_1−C_5 hydrocarbons, in line with the

literature.[10] The highest selectivity to i-C_6 (comprising all branched isomers, such as methyl pentane and dimethylbutane, Figure 7a) was observed at 250 °C for Pt/(H-Beta-25)+Bentonite extrudates. This catalyst at 250 °C temperature also displayed the highest selectivity to dimethylbutane (2,3-dimethylbutane and 2,2-dimethylbutane, Figure 7b) of 7.7% and the highest conversion of *n*-hexane (Figure 6a) of 23.4% compared to other shaped Pt catalysts.

In comparison with other catalysts prepared in the current work, this shaped catalyst with controlled deposition of platinum on beta zeolite has a slightly higher Pt concentration in the whole extrudate volume and the mean Pt particle size as well as the lowest Brønsted and Lewis acidity (Figure 8). On the contrary, for the least active catalyst prepared by postsynthesis, the lowest Pt concentration in the entire extrudate body (i.e., 1.45 wt %, hatched area in Figure 8), the largest particle size, and the highest total acidity were measured.

It was demonstrated for Pt supported on sulfated zirconia[24] that for isomerization of paraffins the highest Lewis acidity is preferred, which could not be confirmed in the current work for Pt composites, containing zeolite beta and bentonite as a binder.

To elucidate the mass transfer in extrudates, we compared the results obtained over Pt/(H-Beta-25)+Bentonite extrudates with the literature data[45] obtained over powder Pt/beta zeolite at similar conditions. Table S5 clearly shows that ca.10-fold higher reaction rate was achieved for Pt/beta powder catalyst obtained under a milder reaction condition (lower Pt loading, lower temperature, atmospheric pressure).

The results displayed in Table S5 indicate that the data generated in the current work are not free from the influence of mass transfer, being thus very relevant for industrial catalysis, where a significant mass transfer is almost unavoidable. It is worth noting that selectivity to the isomers and the 2-methylpentane to 3-methylpentane ratio were maintained, whereas the 2,2-dimethylbutane to 2,3-dimethylbutane ratio was slightly lower for the shaped catalyst.

The conclusions drawn in the literature for *n*-alkanes (n-C_x) hydroisomerization over Pt−zeolite catalysts are mainly related to performance of research catalysts typically with sizes lower than 500 μm. The results obtained in the regime with a limited impact of mass transfer led to conclusions that performance (activity, stability, and selectivity) of bifunctional catalysts containing Pt and a tridimensional large pore zeolite as hydrogenating and acid sites, respectively, depends predominantly on just two parameters, i.e., the ratio of metal to acid

Table 1. Composition of the Product Mixture for *n*-Hexane Transformations over Different Catalysts at 250 °C[a]

catalyst	content of hydrocarbons (wt %)														X (%)		S (%)				2,3-/ 2,2-DMB
	$\sum C_1$–C_4	$\sum C_5$	$\sum C_6$	$\sum C_{7+}$	i-C_5	n-C_5	mc-C_5	c-C_6	2,3-DMB	2,2-DMB	3-MP	2-MP	n-C_6	benzene	n-C_6	benzene	C_6 NAF	i-C_6	DMB	MP	
P	0.11	0.10	99.71	0.07	0.08	0.02	0.41	0.59	0.74	0.22	1.82	3.42	90.63	1.88	8.9	6.8	17.9	57.3	9.9	47.4	3.34
A	0.11	0.06	99.62	0.21		0.06	1.32	1.83		0.07	3.26	5.00	88.15		13.4	100	5.3	52.6	0.1	52.5	
B	0.03	0.02	99.93	0.01		0.02	1.51	1.73	0.29	0.11	4.01	6.18	86.10		14.6	100	1.7	64.4	2.3	62.1	2.67
C	0.02	0.01	99.96	0.01		0.01	1.77	1.43	1.28	0.21	6.55	9.40	79.32		20.7	100	2.2	79.2	6.9	72.3	6.13
D	0.11	0.01	99.87	0.01		0.00	1.81	1.11	1.42	0.41	8.00	12.54	74.58		23.4	100	8.3	92.6	7.7	84.9	3.49

[a]P, 100% H-Beta-25 (CP814E, powder); A, Pt/(H-Beta-25+Bentonite), 2% Pt extrudate (in situ synthesis); B, Pt/(H-Beta-25+Bentonite)+H-Beta-25, 2% Pt extrudate (in situ synthesis); C, Pt/(Bentonite), 2% Pt extrudate (post synthesis); D, Pt/(H-Beta-25)+Bentonite, 2% Pt extrudate (in situ synthesis); i-, isomers; mc-, methylcyclo-; c-, cyclo-; DMB, dimethylbutane; MP, methylpentane; C$_6$ NAF, C$_6$ naphthene ring opening.

sites c_{Pt}/c_A, and the proximity of both sites to each other.[2,3,7,11,13,15]

This c_{Pt}/c_A ratio was extremely different (from 0.07 to 1.12, Figure 8) for shaped Pt catalysts tested in the current work with the same starting composition and nominal loading, prepared, however, via different preparation methods including deposition of Pt on the extrudates. It is generally known that an ideal bifunctional catalyst is obtained when the metal to acid sites ratio has to be high enough to reach a certain plateau, where the reactions on acid sites are rate-limiting.[2,3,7,11,13,15] Following this concept, a high c_{Pt}/c_A is considered necessary to obtain the optimal performance. For low values of c_{Pt}/c_A (<0.03), the activity per acid site is low, deactivation is rapid, and a straight alkane is directly transformed to all isomerization and cracking products. For high values (≥0.17), the activity per acid site is maximal, deactivation is very slow, and n-C$_x$ is converted into monobranched, dibranched, and tribranched isomers as well as cracking products.[2,3,7,15,46]

To experimentally verify a potential impact of deactivation and catalyst stability, a few short-term runs for 3 h were done for the catalyst with the lowest c_{Pt}/c_A ratio at the highest temperatures. The catalytic performance was stable without showing any influence on activity or selectivity.

In agreement with the reasoning above, catalytic activity (Figure 9a) and isomerization selectivity (Figure 9b) increased with increasing the metal to acid sites ratio also in the case of extruded Pt catalysts. However, it should be noted that at high temperature, too high conversion level (ca. 100%) prevents a meaningful analysis on the influence of c_{Pt}/c_A ratio. In the case of low temperature the plateau was not reached even for a very high c_{Pt}/c_A ratio of 1.12.

For many years, proximity of metal and acid sites was considered as a key parameter of an "ideal" bifunctional catalyst, quantified through the Weisz Intimacy Criterion.[3,7,11,13,15] Specifically, many studies in the literature have shown that the maximal intimacy between the metal and acid sites enhances selectivity to skeletal isomers.[3,7,11,15,47] However, recent reports reopened the debate about the ideal proximity between both functions for optimal performances[2,13] considering not only activity but also selectivity and resistance to deactivation. Zecevic et al.[13] reported closer distances between the two functions as being detrimental to the isomerization selectivity, whereas in the work of Gutierrez-Acebo et al.,[2] no influence of the distance between both functions on catalytic performance was observed up to a micrometer scale.

Figure 10 displays a schematic view on the catalysts employed in this study, presenting different degrees of intimacy between the metal and acid sites. From this scheme and literature data,[2,13] it can be assumed that the shortest distances between Pt (black points) and acidic sites (gray circles) are in Pt/(H-Beta-25)+Bentonite (Figure 10a), where platinum is deposited exclusively on beta zeolite. Conversely, the longest distances can be expected for Pt/(H-Beta-25+Bentonite) prepared via the post synthesis (Figure 10d), where Pt is deposited randomly in the outer layer occupying ca. 17.4% of the whole extrudates volume. Therefore, it can be suggested that the degree of intimacy between the metal and acid sites is ranked as follows: Pt/(H-Beta-25) with nanoscale distance[2,13] > Pt/(H-Beta-25+Bentonite) with uniform Pt distribution in the whole extrudate (70% in nanoscale distance and 30% in macroscale distance) > Pt/(Bentonite) in
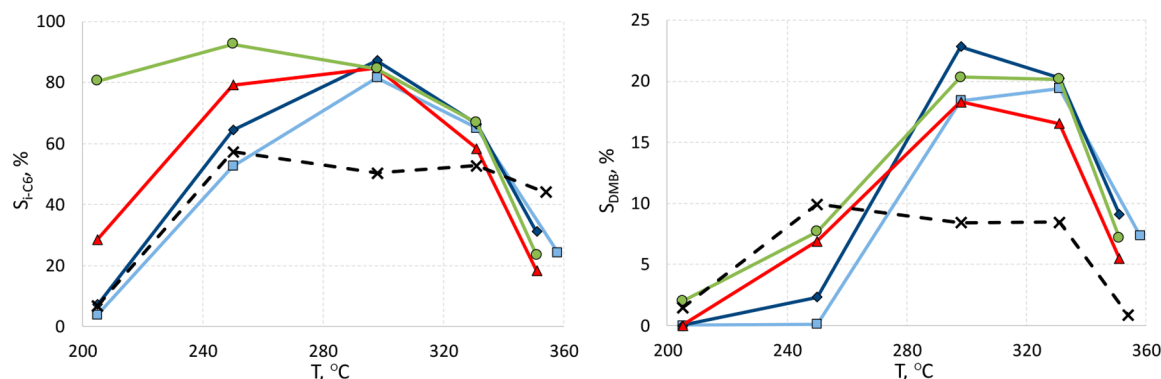
Figure 7. (a) Selectivity of C_6 isomers as a function of temperature; (b) dibranched isomers selectivity as a function of temperature. Symbols: ×, 100% H-Beta-25 (CP814E, powder); ■, Pt/(H-Beta-25+Bentonite), 2% Pt extrudate (post synthesis); ◆, Pt/(H-Beta-25+Bentonite), 2% Pt extrudate (in situ synthesis); ▲, Pt/(Bentonite)+H-Beta-25, 2% Pt extrudate (in situ synthesis); ●, Pt/(H-Beta-25)+Bentonite, 2% Pt extrudate (in situ synthesis).
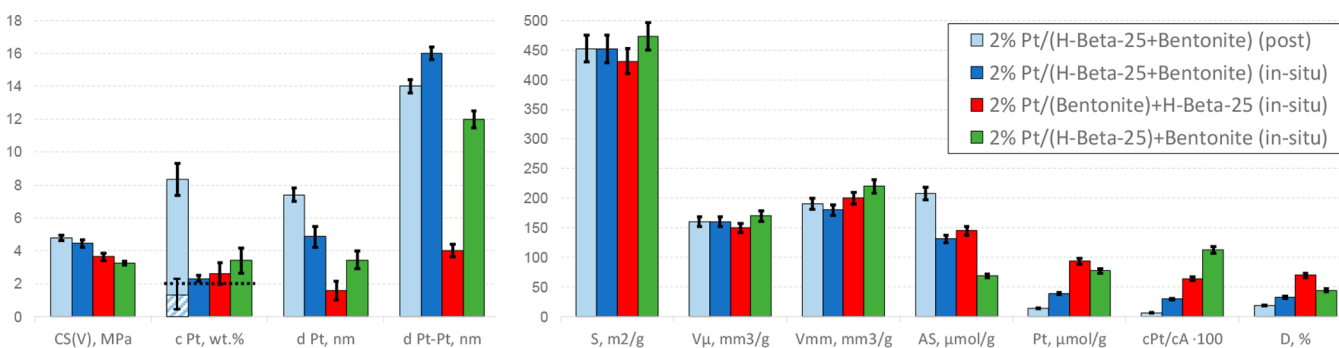

Figure 8. Characterization data for Pt extrudates. Legend: CS(V), crushing strength of extrudates in vertical position; c_{Pt}, platinum concentration on the top of extrudates; d Pt, particle size of platinum; d_{Pt-Pt}, the average shortest distance between Pt sites (determined by TEM); S, specific surface area; Vμ, micropore volume; V_{mm}, meso-and macropore volume; AS, total acid sites; Pt, platinum concentration in the entire volume of extrudates; c_{Pt}/c_A, metal-to-acid site ratio; D, dispersion of Pt. Error bars correspond to the standard deviation of the data.
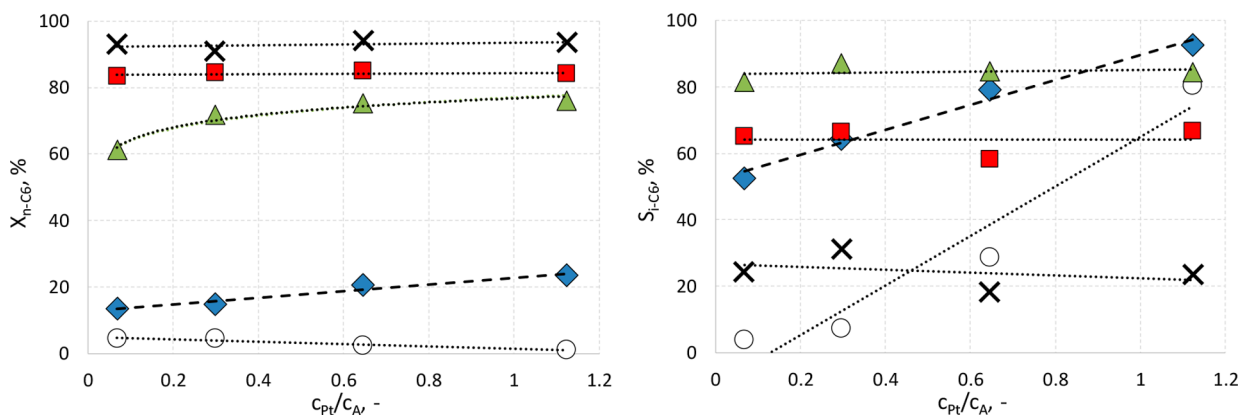

Figure 9. Isomerization of *n*-hexane as a function of c_{Pt}/c_A ratio (a) conversion; (b) selectivity to C_6 isomers. Legend: ○, 200 °C; ◆, 250 °C; ▲, 300 °C; ■, 330 °C; ×, 350 °C.
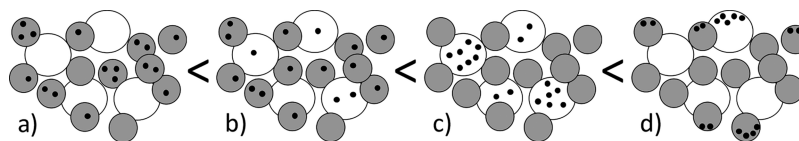

Figure 10. A schematic picture of the catalysts employed in this study, showing different distances between the metal and acid sites: (a) Pt/(H-Beta-25)+Bentonite, 2% Pt extrudate (in situ synthesis); (b) Pt/(H-Beta-25+Bentonite), 2% Pt extrudate (in situ synthesis); (c) Pt/(Bentonite)+H-Beta-25, 2% Pt extrudate (in situ synthesis); (d) Pt/(H-Beta-25+Bentonite), 2% Pt extrudate (post synthesis). Legend: H-Beta-25 (gray circle), bentonite (white circle), Pt (black dots).
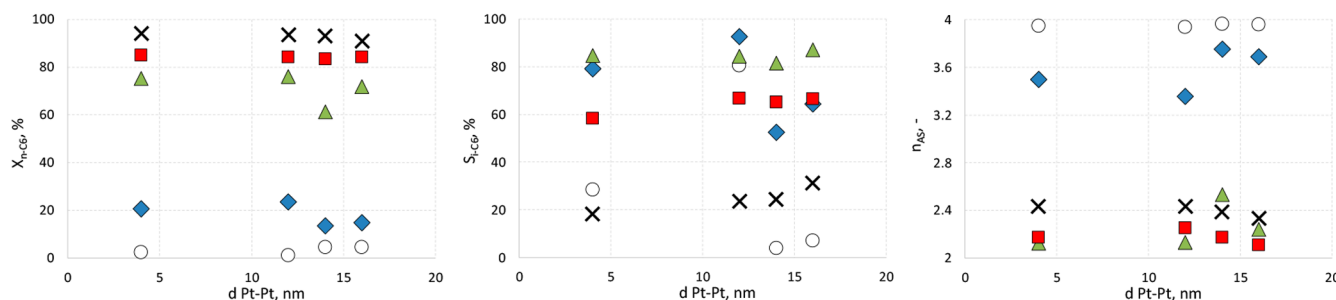
Figure 11. Isomerization of *n*-hexane as a function of Pt–Pt distance: (a) conversion; (b) selectivity to C_6 isomers; (c) the average number of acid steps (n_{AS}). Legend: ○, 200 °C; ◆, 250 °C; ▲, 300 °C; ■, 330 °C; ✕, 350 °C.

microscale distance[2,13] > Pt/(H-Beta-25+Bentonite) with Pt concentrated in the extrudate outer layer.

At low temperatures (below 300 °C), extrudates with the closest degree of intimacy between the metal and acid sites achieved the best results in terms of *n*-hexane conversion and C_6 isomers selectivity (Figure 9). This is apparently clear for the data generated at 250 °C, where much worse results in terms of both activity and selectivity were obtained over the catalyst exhibiting the worst proximity. At higher temperature, differences in the performance were less prominent. At 330 °C, conversion was almost the same for all catalysts, giving similar selectivity to C6 isomers. Absence of any clear trend in activity and selectivity can be seen from Figure 9 for the data obtained at the highest temperature. However, at least for the experimental data in the temperature domain of 200–300 °C, it can be stated that the catalytic behavior increased with increasing proximity.

Another important parameter can be the metal site density (Me–Me distance). In n-C_x transformation,[3,11,15] it was shown that the number of acid sites encountered by the olefinic intermediates during their diffusion between two Pt sites (generally along the zeolite micropores) had to be such that they undergo only one skeletal transformation. Balatha et al.[11] remarked that this number should significantly depend on the degree of intimacy between Pt and acid sites; however, no quantification of this number was proposed.

Figure 11 shows the effect of Pt sites density on conversion of *n*-hexane, selectivity to C_6 isomers and the average number of acid steps involved in the transformation of one n-C_6 molecule (n_{AS}). This number of acid steps (n_{AS}) was estimated from the initial product distribution (mono branched isomers, MB; di branched isomers, DB; isomers and cracking products, IC).[3,11] As the initial molar (weight) distribution over Pt/(H-Beta-25)+Bentonite extrudates at 250 °C is MB, 0.21; DB, 0.018; and IC, 0.78; the value of n_{AS} was equal to $0.21 \times 1 + 0.018 \times 2.5 + 0.78 \times 4 = 3.36$, which means that over this catalyst, the transformation of each n-C_6 molecule requires an average number of ~3.4 acid steps.

In all cases, it was revealed that the Pt–Pt distance had a negligible effect on the catalytic behavior. This result is different from the literature study,[11] where it was stated that the n_{AS} value significantly increases with increasing the distance between Pt sites in powder catalysts (in micrometer scale).

In summary, for the reference temperature of 250 °C (Table S6), the key parameter governing activity and selectivity of bifunctional shaped Pt catalyst appears to be the metal/acid balance rather than the metal site density (Pt–Pt distance). Just this c_{Pt}/c_A ratio was significantly influenced by the

preparation method of shaped catalysts, including the way Pt is deposited on the extrudates.

4. CONCLUSIONS

This work aimed at shedding light on the parameters to be controlled during the scale-up of bifunctional catalysts from powder to shaped bodies. Establishing correlations between the physicochemical (surface, structural, textural, and morphological) and catalytic characteristics of shaped Pt catalysts could significantly contribute to the design of an "ideal" (highly active, stable, and selective) bifunctional shaped catalyst that is indispensable to developing cleaner processes of industrial relevance.

Four different shaped catalysts in the form of extrudates with a controlled deposition of platinum in different locations in the final extrudates and the same composition were prepared, altering the sequence of the following steps for preparation of zeolite–binder composites: Pt impregnation on the zeolite, binder, or the extrudate and extrusion per se. Different variations of the synthesis steps were used to prepare four different types. All catalysts were synthesized with the 70:30 ratio of H-Beta-25:bentonite and with a Pt nominal loading of 2 wt % in the final extrudates.

The catalysts were characterized by a range of physicochemical methods. Activity and selectivity of catalysts in isomerization of *n*-hexane containing 1% benzene were evaluated in a fixed bed reactor.

This study revealed that various ways of Pt deposition on the extrudates strongly effected the metal-to-acid site ratio (from 0.07 to 1.12). At low temperatures (250 °C), this ratio is a key parameter in determining activity and selectivity of the metal/acid bifunctional shaped catalysis similar to powder catalysts.

Pt extrudates exhibited a decrease in the total acid sites as compared to pristine H-Beta-25 extrudates. The binder presence decreased the acidic properties of a zeolite as a result of changes in the solid-state ion exchange between zeolite protons and clay sodium. The morphology, Pt particle size, total acidity, and strength of the shaped catalysts were strongly influenced by the preparation method, whereas the textural properties were comparable. A decrease in Pt particle size due to extrusion was observed in all types of extrudate. Eggshell and uniformly distributed Pt catalysts were prepared via the post synthesis and in situ synthesis methods, respectively. All extrudates were devoid of structural defects after the reaction.

The highest conversion of *n*-hexane and selectivity to C_6 isomers (comprising all branched isomers, such as methyl pentane and dimethylbutane) was obtained with extrudates prepared via in situ synthesis with platinum located on the

zeolite. The extrudates prepared in this way have the highest metal-to-acid site ratio and closest proximity, displaying at the same time somewhat lower but still acceptable mechanical strength.

■ ASSOCIATED CONTENT

Ⓢ Supporting Information

The Supporting Information is available free of charge on the ACS Publications website at DOI: 10.1021/acs.iecr.9b01931.

> Catalyst characterization: elemental analysis, X-ray map of Pt, whole extrudates and longitudinal cross-section, SEM images, TEM images, textural properties, acidity, mechanical strength of extrudates; calculations of conversion and selectivity; hydroisomerization of n-hexane over powder catalyst (PDF)

■ AUTHOR INFORMATION

Corresponding Author
*Email: dmurzin@abo.fi.

ORCID ⓘ
Dmitry Yu. Murzin: 0000-0003-0788-2643

Notes
The authors declare no competing financial interest.

■ ACKNOWLEDGMENTS

■ REFERENCES

(1) Mendes, P. S. F.; Silva, J. M.; Ribeiro, M. F.; Daudin, A.; Bouchy, C. From Powder to Extrudate Zeolite-Based Bifunctional Hydroisomerization Catalysts: on Preserving Zeolite Integrity and Optimizing Pt Location. *J. Ind. Eng. Chem.* **2018**, *62*, 72.

(2) Gutierrez-Acebo, E.; Leroux, C.; Chizallet, C.; Schuurman, Y.; Bouchy, C. Metal/Acid Bifunctional Catalysis and Intimacy Criterion for Ethylcyclohexane Hydroconversion: When Proximity Does Not Matter. *ACS Catal.* **2018**, *8*, 6035.

(3) Batalha, N.; Pinard, L.; Pouilloux, Y.; Guisnet, M. Bifunctional Hydrogenating/Acid Catalysis: Quantification of the Intimacy Criterion. *Catal. Lett.* **2013**, *143*, 587.

(4) Primo, A.; Garcia, H. Zeolites as Catalysts in Oil Refining. *Chem. Soc. Rev.* **2014**, *43*, 7548.

(5) Sahu, R.; Song, B. J.; Im, J. S.; Jeon, Y. P.; Lee, C. W. A Review of Recent Advances in Catalytic Hydrocracking of Heavy Residues. *J. Ind. Eng. Chem.* **2015**, *27*, 12.

(6) Weitkamp, J. Catalytic Hydrocracking-Mechanisms and Versatility of the Process. *ChemCatChem* **2012**, *4*, 292.

(7) Alvarez, F.; Ribeiro, F. R.; Perot, G.; Thomazeau, C.; Guisnet, M. Hydroisomerization and Hydrocracking of Alkanes - Influence of the Balance Between Acid and Hydrogenating Functions on the Transformation of n-Decane on PtHY Catalysts. *J. Catal.* **1996**, *162*, 179.

(8) Maxwell, I. E.; Naber, J. E.; Dejong, K. P. The Pivotal Role of Catalysis in Energy-Related Environmental Technology. *Appl. Catal., A* **1994**, *113*, 153.

(9) Stojkovic, N.; Vasic, M.; Marinkovic, M.; Randjelovic, M.; Purenovic, M.; Putanov, P.; Zarubica, A. A Comparative Study of n-Hexane Isomerization over Solid Acids Catalysts: Sulfated and Phosphated Zirconia. *Chem. Ind. Chem. Eng. Q.* **2012**, *18*, 209.

(10) Chuparev, E. V.; Zernov, P. A.; Parputs, O. I.; Lisitsyn, N. V. Low Temperature Isomerization of n-Hexane on Catalyst Systems $Al_2O_3/ZrO_2/SO_4/Pt$. *Russ. J. Appl. Chem.* **2014**, *87*, 767.

(11) Batalha, N.; Pinard, L.; Bouchy, C.; Guillon, E.; Guisnet, M. n-Hexadecane Hydroisomerization over Pt-HBEA Catalysts. Quantification and Effect of the Intimacy between Metal and Protonic Sites. *J. Catal.* **2013**, *307*, 122.

(12) Sousa, B. V.; Brito, K. D.; Alves, J. J. N.; Rodrigues, M. G. F.; Yoshioka, C. M. N.; Cardoso, D. n-Hexane Isomerization on Pt/HMOR: Effect of Platinum Content. *React. Kinet., Mech. Catal.* **2011**, *102*, 473.

(13) Zecevic, J.; Vanbutsele, G.; de Jong, K. P.; Martens, J. A. Nanoscale Intimacy in Bifunctional Catalysts for Selective Conversion of Hydrocarbons. *Nature* **2015**, *528*, 245.

(14) Akhmedov, V. M.; Al-Khowaiter, S. H. Recent Advances and Future Aspects in the Selective Isomerization of High n-Alkanes. *Catal. Rev.: Sci. Eng.* **2007**, *49*, 33.

(15) Guisnet, M.; Magnoux, P. Coking and Deactivation of Zeolites - Influence of the Pore Structure. *Appl. Catal.* **1989**, *54*, 1−27.

(16) de Lucas, A.; Sanchez, P.; Funez, A.; Ramos, M. J.; Valverde, J. L. Liquid-Phase Hydroisomerization of n-Octane over Platinum-Containing Zeolite-Based Catalysts with and without Binder. *Ind. Eng. Chem. Res.* **2006**, *45*, 8852.

(17) Whiting, G. T.; Meirer, F.; Mertens, M. M.; Bons, A. J.; Weiss, B. M.; Stevens, P. A.; de Smit, E.; Weckhuysen, B. M. Binder Effects in SiO_2- and Al_2O_3-Bound Zeolite ZSM-5-Based Extrudates as Studied by Microspectroscopy. *ChemCatChem* **2015**, *7*, 1312.

(18) Dorado, F.; Romero, R.; Canizares, P. Hydroisomerization of n-Butane over Pd/HZSM-5 and Pd/H Beta with and without Binder. *Appl. Catal., A* **2002**, *236*, 235.

(19) Jasra, R. V.; Tyagi, B.; Badheka, Y. M.; Choudary, V. N.; Bhat, T. S. G. Effect of Clay Binder on Sorption and Catalytic Properties of Zeolite Pellets. *Ind. Eng. Chem. Res.* **2003**, *42*, 3263.

(20) Dorado, F.; Romero, R.; Canizares, P. Influence of Clay Binders on the Performance of Pd/HZSM-5 Catalysts for the Hydroisomerization of n-Butane. *Ind. Eng. Chem. Res.* **2001**, *40*, 3428.

(21) Ozcan, A.; Kalipcilar, H. Preparation of Zeolite A Tubes from Amorphous Aluminosilicate Extrudates. *Ind. Eng. Chem. Res.* **2006**, *45*, 4977.

(22) Vajglova, Z.; Kumar, N.; Peurla, M.; Peltonen, J.; Heinmaa, I.; Murzin, D. Y. Synthesis and Physicochemical Characterization of Beta Zeolite-Bentonite Composite Materials for Shaped Catalysts. *Catal. Sci. Technol.* **2018**, *8*, 6150.

(23) Liu, H.; Zhou, Y. M.; Zhang, Y. W.; Bai, L. Y.; Tang, M. H. Influence of Binder on the Catalytic Performance of PtSnNa/ZSM-5 Catalyst, for Propane Dehydrogenation. *Ind. Eng. Chem. Res.* **2008**, *47*, 8142.

(24) Devyatkov, S. Y.; Zinnurova, A. Al; Aho, A.; Kronlund, D.; Peltonen, J.; Kuzichkin, N. V.; Lisitsyn, N. V.; Murzin, D.Yu. Shaping of Sulfated Zirconia Catalysts by Extrusion: Understanding the Role of Binders. *Ind. Eng. Chem. Res.* **2016**, *55*, 6595.

(25) Baldovino-Medrano, V. G.; Alcazar, C.; Colomer, M. T.; Moreno, R.; Gaigneaux, E. M. Understanding the Molecular Basics behind Catalyst Shaping: Preparation of Suspensions of Vanadium-Aluminum Mixed (Hydr)Oxides. *Appl. Catal., A* **2013**, *468*, 190.

(26) Chi, K.; Zhen, Z.; Zhijian, T.; Sheng, H.; Lijun, Y.; Thianshu, L.; Bingchun, W.; Xiangbin, M.; Shanbin, G.; Mingwei, T.; Yanfeng, L. Hydroisomerization Performance of Platinum Supported on ZSM-22/ZSM-23 Intergrowth Zeolite Catalyst. *Pet. Sci.* **2013**, *10*, 242.

(27) Geng, C.-H.; Zhang, F.; Gao, Z.-X.; Zhao, L-Fu.; Zhou, J.-L. Hydroisomerization of n-Tetradecane over Pt/SAPO-11 Catalyst. *Catal. Today* **2004**, *93−95*, 485.

(28) Ramos, M. J.; Gómez, J. P.; Dorado, F.; Sánchez, P.; Valverde, J. L. Hydroisomerization of a Refinery Naphtha Stream over Platinum Zeolite-Based Catalysts. *Chem. Eng. J.* **2007**, *126*, 13.

(29) Ghebre-Selassie, I.; Martin, C. *Pharmaceutical Extrusion Technology*; CRC Press, 2003.

(30) ImageJ program, https://imagej.net/Welcome (accessed April 2019).

(31) Horvath, G.; Kawazoe, K. Method for the Calculation of Effective Pore-Size Distribution in Molecular-Sieve Carbon. *J. Chem. Eng. Jpn.* **1983**, *16*, 470.

(32) Emeis, C. A. Determination of Integrated Molar Extinction Coefficients for Infrared-Adsorption Bands of Pyridine Adsorbed on Solid Acid Catalysts. *J. Catal.* **1993**, *141*, 347.

(33) Pariente, M. I.; Martinez, F.; Botas, J. A.; Melero, J. A. Extrusion of Fe_2O_3/SBA-15 Mesoporous Material for Application as Heterogeneous Fenton-like Catalyst. *Aims Env. Sci.* **2015**, *2*, 154.

(34) Delmon, B.; Grange, P.; Jacobs, P. A.; Poncelet, G. *Scientific Bases for the Preparation of Heterogeneous Catalysts, in Preparation of Catalysts II*; Elsevier Science, 1977.

(35) Ji, Y.; van der Eerden, A.; Koot, V.; Kooyman, P. J.; Meeldijk, J. D.; Weckhuysen, B. M.; Koningsberger, D. C. Influence of support ionicity on the hydrogen chemisorption of Pt particles dispersed in Y zeolite: consequences for Pt particle size determination using the H/M method. *J. Catal.* **2005**, *234*, 376.

(36) Choudhary, V. R.; Devadas, P.; Kinage, A. K.; Guisnet, M. Influence of Binder on the Acidity and Performance of H-Gallosilicate (MFI) Zeolite in Propane Aromatization. *Appl. Catal., A* **1997**, *162*, 223.

(37) Romero, M. D.; Calles, J. A.; Rodriguez, A.; deLucas, A. Acidity Modification During the Agglomeration of ZSM-5 with Montmorillonite. *Microporous Mater.* **1997**, *9*, 221.

(38) Choudhary, V. R.; Nayak, V. S. Effect of Degree of H^+ Exchange on the Acidity Distribution of HNA-ZSM-5. *Zeolites* **1985**, *5*, 15.

(39) Hernando, H.; Ochoa-Hernández, C.; Shamzhy, M.; Moreno, I.; Fermoso, J.; Pizarro, P.; Coronado, J. M.; Čejka, J.; Serrano, D. P. The crucial role of clay binders in the performance of ZSM-5 based materials for biomass catalytic pyrolysis. *Catal. Sci. Technol.* **2019**, *9*, 789.

(40) Kubicka, D.; Kumar, N.; Venalainen, T.; Karhu, H.; Kubickova, I.; Osterholm, H.; Murzin, D.Yu. Metal-Support Interactions in Zeolite-Supported Noble Metals: Influence of Metal Crystallites on the Support Acidity. *J. Phys. Chem. B* **2006**, *110*, 4937.

(41) Lefevere, J.; Protasova, L.; Mullens, S.; Meynena, V. 3D-Printing of Hierarchical Porous ZSM-5: The Importance of the Binder System. *Mater. Des.* **2017**, *134*, 331.

(42) Hareesh, U. N. S.; Anantharaju, R.; Biswas, P.; Rajeswari, K.; Johnson, R. Colloidal Shaping of Alumina Ceramics by Thermally Induced Gelation of Methylcellulose. *J. Am. Ceram. Soc.* **2011**, *94*, 749.

(43) Serrano, D. P.; Sanz, R.; Pizarro, P.; Moreno, I.; de Frutos, P.; Blazquez, S. Preparation of Extruded Catalysts Based on TS-1 Zeolite for their Application in Propylene Epoxidation. *Catal. Today* **2009**, *143*, 151.

(44) Lee, K. Y.; Lee, H. K.; Ihm, S. K. Influence of Catalyst Binders on the Acidity and Catalytic Performance of HZSM-5 Zeolites for Methanol-to-Propylene (MTP) Process: Single and Binary Binder System. *Top. Catal.* **2010**, *53*, 247.

(45) van de Runstraat, A.; Kamp, J. A.; Stobbelaar, P. J.; van Grondelle, J.; Krijnen, S.; van Santen, R. A. Kinetics of Hydro-Isomerization of n-Hexane over Platinum Containing Zeolites. *J. Catal.* **1997**, *171*, 77.

(46) Guisnet, M. Ideal" Bifunctional Catalysis over Pt-Acid Zeolites. *Catal. Today* **2013**, *218*, 123.

(47) Eley, D. D.; Selwood, P. W.; Weisz, P. B.; Balandin, A. A.; De Boer, J. H.; Debye, P. J.; Emmett, P. H.; Horiuti, J.; Jost, W.; Natta, G.; Rideal, E. K.; Taylor, H. S. *Advances in Catalysis*; Academic Press, 1962; Vol. *13*.